Electronic Supplementary Material (ESI) for Analyst.

Electronic Supplementary Information

On-line visualization of multicolor chemical images with stimulated Raman scattering spectral microscopy

Yoichi Otsuka, *[ac] Koji Makara,[a] Shuya Satoh,[a] Hiroyuki Hashimoto[a] and Yasuyuki Ozeki[b]

[a] Frontier Research Center, Canon Inc., 30-2 Shimomaruko 3-chome, Ohta-ku, Tokyo 146-8501, Japan.

[b] Department of Electrical Engineering and Information System, The University of Tokyo, 7-3-1 Hongo, Bunkyo-ku, Tokyo 113-8656, Japan

[c] Present address: Department of Chemistry, Graduate School of Science, Osaka University, Toyonaka, Osaka 560-0043, Japan. E-mail: otsuka@chem.sci.osaka-u.ac.jp

* Corresponding author

Contents

S-1. Data acquisition and visualization system

The high-speed stimulated Raman scattering (SRS) microscope and its experimental setup have been described in detail in a previous report[i]. The difference from the previous setup is the use of the auto stage (MLS203-1, Thorlabs) and the microscope housing (IX73, Olympus).

The field-programmable gate array (FPGA)-1 (PXIe-7966R, National Instruments) for the data acquisition was connected to the analog-to-digital converter (ADC) (NI 5734, National Instruments). The SRS signal from the lock-in amplifier was input to the ADC. The horizontal and vertical synchronizing signal (HSYNC and VSYNC) from the homemade scanner controller was also input to the ADC. An XY scanner was used for laser scanning. The fast axis was scanned with a resonant scanner (RS) (CRS 8 kHz, GSI) and the slow axis was scanned with a galvano scanner. Because the displacement of the laser spot by RS was similar to a sine curve, an unequally spaced pixel clock was generated to correct the laser scanning. The SRS signal at the pixel clock was transferred to FPGA-1 after HSYNC. Because the backward and forward motions of the RS were used for the odd and even lines of the SRS image, respectively, the SRS data for the even lines was inverted for the SRS image in FPGA-1. After the data for the SRS image (500 × 500 pixels) was obtained, it was transferred to the computer memory by direct memory access. FPGA-2 (PXIe-7852R, National Instruments) equipped with a digital-to-analog converter (DAC) was connected to the spectral filter. An arbitrary DC voltage equipped with a digital-to-analog converter (DAC) was input to the galvano scanner of the filter. The timing of the voltage output was synchronized to the HSYNC. The value of the bias voltage was determined by the Raman shift for each measurement. The operation clock of both FPGAs was 120 MHz and it was also synchronized to the 10 MHz clock from the stage controller. The 10 MHz clocks are synchronized to the velocity signal of the RS that oscillates around 8 kHz.

The SRS image of different Raman shifts was reconstructed in the computer memory (PXIe-8135, National Instruments) to form the data array of n lines and m + 1 columns where n and m correspond to the number of the Raman shift and the number of pixels, respectively. A background image, which reflects the offset voltage of the lock-in amplifier, was also obtained after the m^{th} Raman shift image. To obtain background images, the output of the YbF laser was cut off to suppress SRS signals. The background noise level was used for the offset subtraction for principal component analysis (PCA) or independent component analysis (ICA).

The data array was saved to local files and executed by PCA or ICA with other software. The data processing of PCA and ICA was same as previously reported[1]. The array of the score for the n^{th} component was normalized to generate 8-bit bitmap principal component (PC) images. The PC images are named PCn+/PCn-, in which n is the n^{th} principal component and + or – indicates the polarity of the score. The number of components was determined as three for polymer beads,

because there were three kinds of polymer beads. The number of principal components for rat liver tissues was determined as three from the contribution ratio of eigenvalues calculated by PCA with a threshold value of 0.1%. After the ICA, the whitened loading vector and demixing matrix were saved to local files as the preprocessed vectors. The preprocessed vectors were read by the data acquisition software and on-line visualization was executed. The above data acquisition, PCA, ICA and on-line processing of independent component (IC) images were all performed by homemade software (LabVIEW, National Instruments). All Supporting Movies are shrunk by half from the original movies.

S-2. Coloring of PC and IC images and generation of Averaged Raman images

PC and IC images of pre-HSDC was colored red, blue, and green and overlaid by Image J (Rasband, W.S., U.S. National Institute of Health, Bethesda, MD, http://imagej.nih.gov/ij/, 1997-2014.) The brightness and contrast (B&C) was adjusted automatically. The on-line IC images were also colored in the same way as the pre-HSDC images and overlaid.

Averaged Raman images were generated with the Z project function of Image J. The projection type of "average intensity" was used. Before the processing, the HSDC is converted to the multiple Raman images (8-bit BMP files) and they are read by Image J as sequential images. The contrast of averaged Raman images indicates the relative difference of Raman signal intensities at a certain Raman shift range.

S-3. Sample preparation and data acquisition condition

Polymer bead mixture

Polyurethane beads (product type: U, 10 μm average particle diameter, Negami Chemical Industrial Co., Japan), PMMA beads (product type: G, 6 μm average particle diameter, Negami Chemical Industrial Co.), and polystyrene beads (micromer, 10 μm average particle diameter, Corefront, Japan) were dispersed in pure water. Each solution was mixed and put between cover glasses and dried. The sample was also coated with a sealant to prevent the incursion of water used for the water-immersion objective lens. The powers of the Ti:S laser and YbF laser at the input of the laser scanners were 71 and 118 mW, respectively.

The pre-HSDC was obtained for 92 images including 91 different Raman shift images and 1 background image. The Raman shifts were determined at intervals of 3.3 cm^{-1} from 2800 to 3100 cm^{-1}. Ten measurements were averaged in around 30 s. The reduced pre-HSDC was obtained for 10 images including nine different Raman shift images and one background image. The FOV for 92 images (Fig. 2(c)) and 10 images (Fig. 2(e)) were different. The Raman shifts were determined at intervals of 37.5 cm^{-1} from 2800 to 3100 cm^{-1}. Ten measurements were averaged in around 3.3 s.

Rat liver tissue section

A rat liver (Rockland Immunochemicals Inc.) was cryosectioned to a nominal thickness of 100 μm. The tissue section was mounted on a cover glass with phosphate buffered saline (pH 7.4). The sample was sandwiched with a thin cover glass with a thickness of 30 μm. The powers of the Ti:S laser and YbF laser at the input of the laser scanners were 140 and 108 mW, respectively.

The pre-HSDC was obtained for 92 images including 91 different Raman shift images and 1 background image. The Raman shifts were determined at intervals of 3.3 cm^{-1} from 2800 to 3100 cm^{-1}. Twenty measurements were averaged in around 62 s. The reduced pre-HSDC was obtained for seven images, including six different Raman shift images and one background image. The six Raman shifts were 2850, 2900, 2920, 2960, 3010, and 3060 cm^{-1}. Fifty measurements were averaged in around 12 s. The FOV for 92 images (Fig. 3(c)) and 7 images (Fig. 3(e)) were different.

S-4. Fast visualization of rat liver tissue with preprocessed vectors obtained by ICA

The pre-HSDC was processed with PCA-based region of interest (ROI) selection before ICA. This is because IC spectra obtained by ICA was not identical to the Raman spectra of the entire pre-HSDC dataset (Fig. S1). Presumably, this is due to the fact that the quantity of each component varies a lot compared with the case of the mixed polymer beads. The lipid droplets were the minor components in the Raman image, and hence the ICA results are affected by the major components, such as the cytoplasm, nucleus, and sinusoids. Therefore, the pre-HSDC is reconstructed so that the same number of pixels for each component is included. The details of ROI selection have been described previously[ii] and the outline of the selection in this study is shown in Fig. S2.

The pre-HSDC used in Fig. 3 was also used. The pre-HSDC was first analyzed by PCA. All the data points were used for the calculation. The number of components was determined as four from the contribution ratio of eigenvalues calculated by PCA. The PC images (PC*n*+/PC*n*-) were generated by calculating the score for each loading vector. The scores for each PC image were normalized to generate 8-bit bitmap data. In this study, PC2-, PC2+ and PC3- were used. Next, the pixel coordinate with a pixel intensity that matched the selection range were extracted. The extracted pixels were visualized as white, and were used as the ROI. The selection range was adjusted so that the lipid droplets, nucleus and sinusoids, and cytoplasm were appropriately selected. The PC2- images indicated the distribution of the lipid droplets and cytoplasm. The pixel intensity of lipid droplets was higher than that of cytoplasm. The selection range from 30 to 255 enabled us to exclude the cytoplasm signals and extract the pixel coordinates from the lipid droplets. The PC2+ images showed the distribution of the nucleus and sinusoids. The pixel intensity of the nucleus was slightly higher than that of the sinusoids; however, it was difficult to separate them. The selection range was set as 100–255 to select the pixel coordinates with a higher pixel intensity. The PC3- images showed the distribution of the cytoplasm and fiber. As with the PC2+ images, it was difficult to separate them. The selection range was set as 50–255 to select the pixel coordinates with a higher pixel intensity. The number of extracted pixels was 3064, 38,856, and 7409 for PC2-, PC2+, and PC3-, respectively. This result also indicates the area ratio of lipid droplets was 1.16% of the total number of pixels (262,144).

The pixel number of each ROI was adjusted. For each ROI, 3000 pixel coordinate points were selected by random sampling. This process homogenized the pixel number of each component, and hence the lipid droplets, that are the minor components in the pre-HSDC, were treated as the major components because the number of lipid droplets, nucleus, and sinusoid, and cytoplasm were the same, respectively. All the pixel coordinates were combined and used for reconstructing the original pre-HSDC. The dataset of the 512 × 512 × 91 data cube was transformed to a 3 × 3000 × 91 data cube, and analyzed by ICA.

The averaged Raman image and Raman spectra are shown in Figs. S3(a) and (b), respectively. The IC images and IC spectra obtained from the reconstructed pre-HSDC are shown in Figs. S3(c) and (d), respectively. It was confirmed that each IC spectrum was similar to the Raman spectrum (Fig. S3(b)). The overlaid IC image visualized the distribution of cytoplasm (green area) and lipid droplets (red particles). The sinusoid and the nucleus regions were a similar color, although a slight increase in the amount of lipids in the sinusoids was measured (Fig. S3).

The preprocessed vectors obtained by ICA were also applied to new-HSDCs that were obtained in different FOVs. It was confirmed that IC images were displayed immediately after the new-HSDC was obtained (Supporting Movie S4). Because the signal-to-noise ratio was lower than that of the mixed polymer beads, the HSDC was averaged to obtain IC images. When SRS images at 92 Raman shifts were acquired, averaging five times was required to obtain good IC images; however, it took about 15 s to obtain the HSDC. For the faster visualization, the number of image for a HSDC was reduced to seven, including six different Raman images and a background image. As shown in Figs. 3(e) and (f), the IC spectra were similar to the Raman spectra, and the IC images were similar to those in Fig. 3(d). The on-line visualization for the new-HSDC was executed. The data acquisition time was about 2.4 s for averaging 10 times (Supporting Movie S5). Compared with the PCA results, the IC images were noisier, and thus a longer accumulation time was needed.

Figure captions

Figure S1

ICA results of rat liver tissue sections without the PCA-based ROI selection. All the pre-HSDC data were analyzed by ICA. (a) IC spectrum of three components. (b) Overlaid IC image. Compared with Fig. 2(b), each IC spectrum was different from the Raman spectrum of each component in the tissue. In the IC image, each component is visualized as a different color, although the separation of the chemical components is poorer than in Fig. S3.

Figure S2

Data processing with PCA-based ROI selection. (a) PC images and (b) data extraction from PC images of the rat liver section. (c) Data point adjustment by random sampling. (d) Reconstruction of original HSDC.

Figure S3

Hyperspectral SRS imaging and ICA results of rat liver tissue. (a) Averaged Raman image reconstructed for 91 Raman shift images. (b) Raman spectra of cytoplasm, nucleus, and lipid droplets. Each spectrum was obtained for the bead shown in (a). The signal intensity of an area of 11 × 11 pixels was averaged. (c), (d) Overlaid IC images and IC spectra obtained from the HSDC of 92 images. Three IC images that correspond to the IC spectra are shown as red, green, and blue and overlaid. (e), (f) Overlaid IC images and IC spectra obtained from the HSDC of seven images. The Raman spectra shown in (b) are also plotted as dotted lines in (f) for comparison. The intensity of each IC spectrum was normalized to that of the Raman spectra by the linear least-squares method

Figure S1

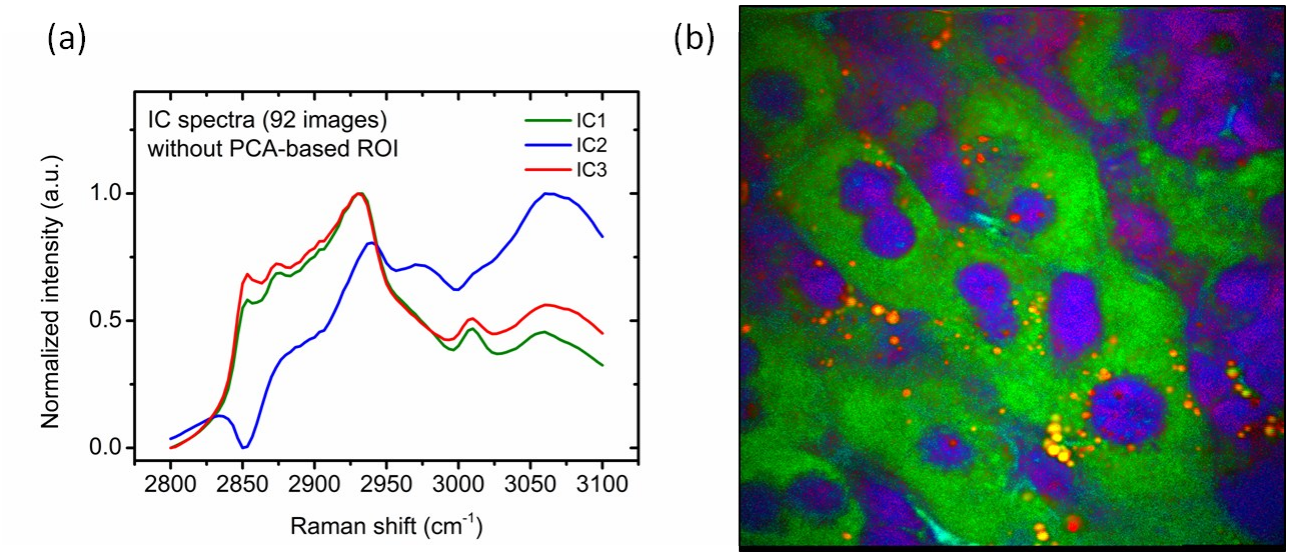
(a)
IC spectra (92 images)
without PCA-based ROI
IC1
IC2
IC3
Normalized intensity (a.u.)
1.0
0.5
0.0
2800
2850
2900
2950
3000
3050
3100
Raman shift (cm-1)
(b)

Figure S2

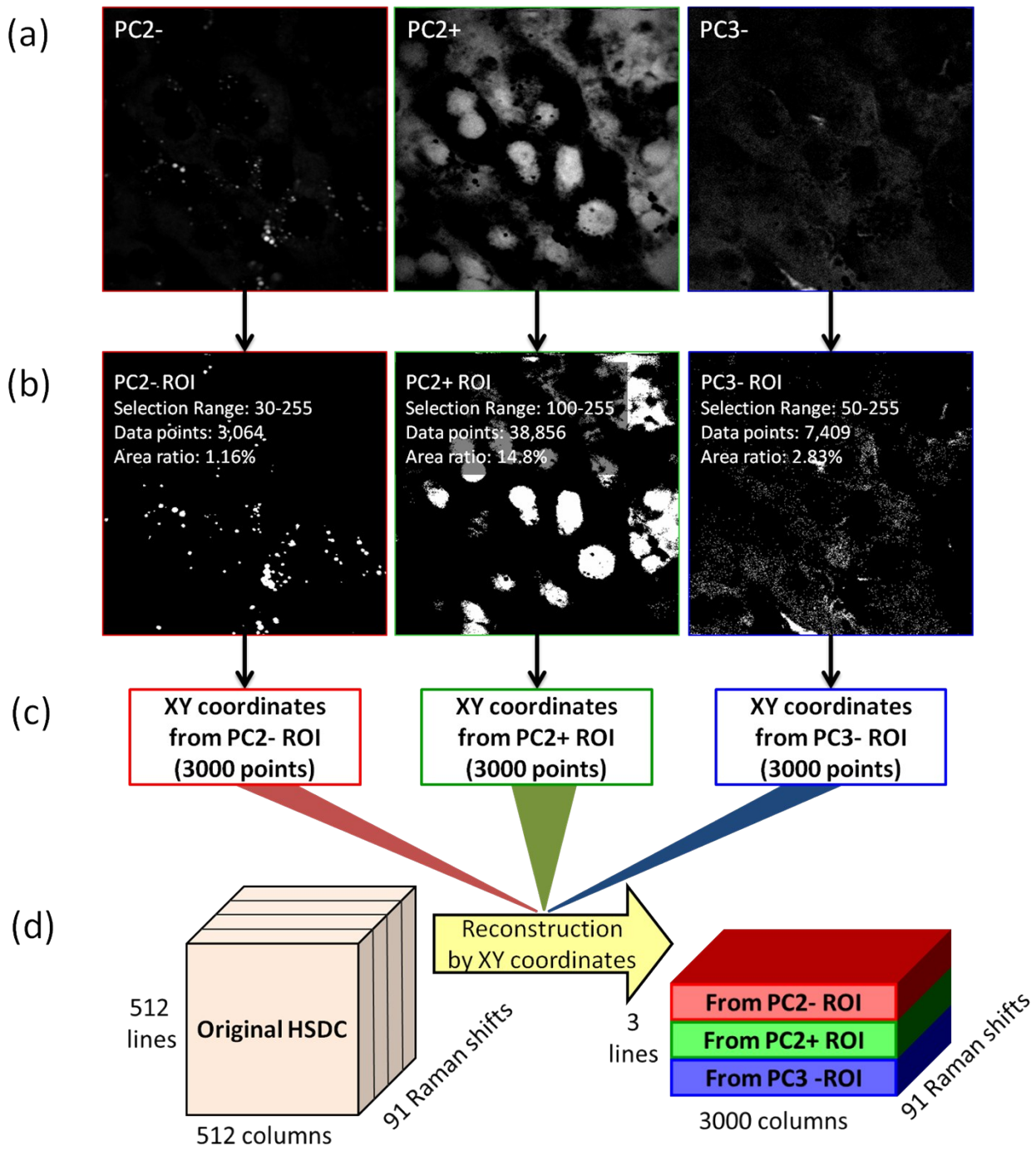
(a)
PC2-
PC2+
PC3-
(b)
PC2- ROI
Selection Range: 30-255
Data points: 3,064
Area ratio: 1.16%
PC2+ ROI
Selection Range: 100-255
Data points: 38,856
Area ratio: 14.8%
PC3- ROI
Selection Range: 50-255
Data points: 7,409
Area ratio: 2.83%
(c)
XY coordinates from PC2- ROI (3000 points)
XY coordinates from PC2+ ROI (3000 points)
XY coordinates from PC3- ROI (3000 points)
(d)
512 lines
Original HSDC
512 columns
91 Raman shifts
Reconstruction by XY coordinates
3 lines
From PC2- ROI
From PC2+ ROI
From PC3 -ROI
3000 columns
91 Raman shifts

Figure S3

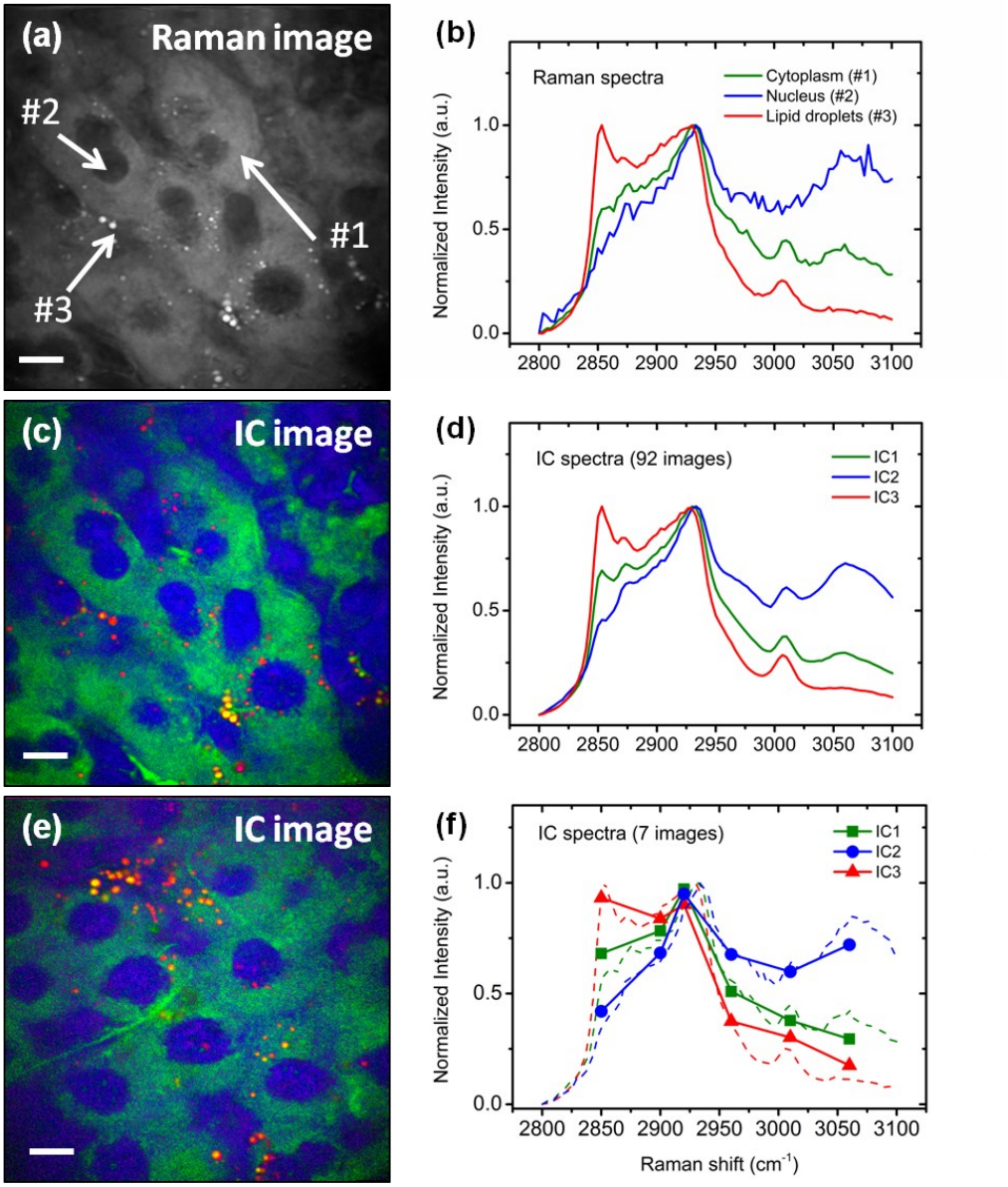
(a)
Raman image
#2
#1
#3
(b)
Raman spectra
Cytoplasm (#1)
Nucleus (#2)
Lipid droplets (#3)
Normalized Intensity (a.u.)
1.0
0.5
0.0
2800 2850 2900 2950 3000 3050 3100
(c)
IC image
(d)
IC spectra (92 images)
IC1
IC2
IC3
Normalized Intensity (a.u.)
1.0
0.5
0.0
2800 2850 2900 2950 3000 3050 3100
(e)
IC image
(f)
IC spectra (7 images)
IC1
IC2
IC3
Normalized Intensity (a.u.)
1.0
0.5
0.0
2800 2850 2900 2950 3000 3050 3100
Raman shift (cm-1)

References

i Y. Ozeki, W. Umemura, Y. Otsuka, S. Satoh, H. Hashimoto, K. Sumimura, N. Nishizawa, K. Fukui, K. Itoh, *Nat. Photonics*, 2012, **6**, 845.

ii Y. Otsuka, S. Satoh, M. Kyogaku, H. Hashimoto, K. Itoh, Y. Ozeki, *Proc. SPIE*, 2014, **8947**, doi: 10.1117/12.2037494.